A Blind Watermarking Scheme Using New Nontensor Product Wavelet Filter Banks

Xinge You, *Senior Member, IEEE*, Liang Du, *Member, IEEE*, Yiu-ming Cheung, *Senior Member, IEEE*, and Qiuhui Chen

***Abstract*—As an effective method for copyright protection of digital products against illegal usage, watermarking in wavelet domain has recently received considerable attention due to the desirable multiresolution property of wavelet transform. In general, images can be represented with different resolutions by the wavelet decomposition, analogous to the human visual system (HVS). Usually, human eyes are insensitive to image singularities revealed by different high frequency subbands of wavelet decomposed images. Hence, adding watermarks into these singularities will improve the imperceptibility that is a desired property of a watermarking scheme. That is, the capability for revealing singularities of images plays a key role in designing wavelet-based watermarking algorithms. Unfortunately, the existing wavelets have a limited ability in revealing singularities in different directions. This motivates us to construct new wavelet filter banks that can reveal singularities in all directions. In this paper, we utilize special symmetric matrices to construct the new nontensor product wavelet filter banks, which can capture the singularities in all directions. Empirical studies will show their advantages of revealing singularities in comparison with the existing wavelets. Based upon these new wavelet filter banks, we, therefore, propose a modified significant difference watermarking algorithm. Experimental results show its promising results.**

***Index Terms*—Nontensor product wavelet filter, singularities, watermarking.**

I. Introduction

With the rapid development of Internet and multimedia technology, how to protect the copyright of products from the illegal usage has been becoming a crucial issue. In general, digital watermarking plays an important role in copyright protection. In the literature, one major kind of watermarking is to embed a watermark imperceptibly into a host image. Since digital products may suffer from a variety of distortions, e.g., JPEG compression, additive noise, cropping, and so on, watermarking algorithms should be robust against these distortions. The robustness means that watermark should be well preserved even if the host image is distorted. Researchers have made the great efforts in developing robust watermarking algorithms [1]–[5]. Basically, the watermark can be embedded in either the spatial domain, or the transform domain. The former embeds a watermark into the host image by directly modifying the pixel value of the host image [6], [7]. In contrast, the latter firstly performs the domain transformation and then embeds a watermarking by modifying the coefficients in transform domain. In general, watermarking in transform domain is more robust than the one in spatial domain. In the past decade, a lot of watermarking algorithms have been developed in transform domain, e.g., discrete cosine transform (DCT) [8].

Besides the DCT, an increasing number of watermarking algorithms [9]–[24] in wavelet domain have been proposed in the literature. For example, Kundur *et al.* [9] employs multiresolution fusion techniques and incorporates a model of the human visual system (HVS) for watermark embedding. It is well known that a watermarking algorithm should largely exploit the nature of HVS. That is, the way that wavelet transform gives a multiresolution representation of images should resemble the procedure of image processing by the human eyes. Nevertheless, the watermarking in [9] is a nonblind watermarking scheme, in which the original image is needed in the watermark extraction phase. In [10], wavelet coefficients of all subbands in the same level are modified according to their relative values. Barni *et al.* [11] utilized the pixel-wise masking in watermark embedding. This method well exploits the similarity between wavelet transform and HVS. Furthermore, as the high frequency subbands of wavelet decomposed images reflect image singularities (e.g., edges and textures), in which a small change is hardly perceptible by human being. Hence, the significant coefficients in high frequency subbands are quite suitable for watermark embedding [13]. For instance, Xia *et al.* [12] added the pseudo-random codes to the large coefficients at high and middle frequency subbands of wavelet decomposed image. Dugad *et al.* [13] embedded the watermarks in wavelet coefficients above a given threshold T_1. Then, another threshold $T_2(T_2 > T_1)$ is utilized for watermark detection. Along this line, it is evidently that the wavelet transform should reveal more singularities so that watermarking in singularities can make a good tradeoff between the two desirable properties of watermarking: robustness and imperceptibility, as stated before. Hence, it is conjectured that the capability of revealing singularities for wavelet determines the performance of the corresponding wavelet-based watermarking.

Manuscript received June 02, 2009; revised January 08, 2010 and May 31, 2010; accepted June 12, 2010. Date of publication June 28, 2010; date of current version November 17, 2010. This work was supported in part by the NSFC under Grants 607731871 and 60973154, the Ministry of Education, China under Grant NCET-07-0338, the Research Grant Council of Hong Kong SAR under Project HKBU 210309, and a Faculty Research Grant of Hong Kong Baptist University (Project Code: FRG2/09-10/098). The associate editor coordinating the review of this manuscript and approving it for publication was Dr. Xuelong Li.

X. You and L. Du are with the Department of Electronics and Information Engineering, Huazhong University of Science and Technology, Hongshan, Wuhuan, Hubei 430074, China (e-mail: you1231cncn@yahoo.com.cn; liang.du.hust@gmail.com).

Y. Cheung is with the Department of Computer Science, Hong Kong Baptist University, Kowloon, Hong Kong (e-mail: ymc@comp.hkbu.edu.hk).

Q. Chen is with the School of Informatics, Guangdong University of Foreign Studies Telephone, Guangzhou, Guangdong 510090, China (e-mail: chenqiuhui@hotmail.com).

Color versions of one or more of the figures in this paper are available online at http://ieeexplore.ieee.org.

Digital Object Identifier 10.1109/TIP.2010.2055570

More recently, some sophisticated wavelet domain watermarking schemes have been proposed. For instance, Wang *et al.* [19] proposed a watermarking algorithm in wavelet domain by adopting different threshold values in different DWT subimages [i.e., multithreshold wavelet coder (MTWC)]. Since this approach is compatible with the evolution of the distortion distribution in each subimage as image data are compressed in the embedded coding process, its error rate is relatively low. Nevertheless, this method is not desirable because it is nonblind watermarking [19]. In [16]–[18], and [20], watermarks are embedded according to the wavelet tree structure. Specifically, Hsieh *et al.* [17] embedded watermark based upon the qualified significant wavelet tree (QSWT), in which watermark was embedded in Level 2 and Level 3 high-frequency subimages. Wang and Lin [20] have made use of the wavelet trees in such a way that they selectively discarded the least significant bits (LSB) of wavelet trees. In this method, an original image is decomposed into the three levels and then each two so-called super trees are utilized to embedded one watermark bit. By comparing values of LSB bits of each super tree group, watermark can be extracted. Nevertheless, the inconsistence of error accumulation between encoder and decoder may aggravate the watermark distinction [18]. Furthermore, [16] has applied the idea of DEW [25], a methodology derived from DCT domain watermarking, to design robust watermarking algorithm in wavelet domain, in which watermark is embedded by differentiating the energy of cross blinding wavelet trees (CBWT). Compared with [20], CBWT has the smaller energy rate which is more suitable for differentiation (i.e., suitable to create energy differences). By setting a threshold T to ensure the fidelity of watermarked image, paper [16] has achieved a good tradeoff between the fidelity and robustness. However, a large number of wavelet coefficients are not suitable for watermark embedding [16], thus, the corresponding capacity is very limited. Lin *et al.* [21] have developed a wavelet domain watermarking scheme by embedding watermarks blockwise, in which every seven nonoverlapped wavelet coefficients of host image are grouped into a block by analyzing the distribution of wavelet coefficients with the consideration of watermarking capacity. Then, the difference of the two largest wavelet coefficients (i.e., significant coefficients) in each group is modified according to the watermark bit to be embedded. In the extracting phase, the extracting threshold is adaptively selected based upon the distribution of all significant differences of a watermarked image. Experimental results show that this algorithm is quite robust against the distortions. Evidently, the performance of this scheme is closely related to the significant difference. Unfortunately, significant difference in this scheme is not so desirable because of traditional wavelet's limitations on revealing singularities. Subsequently, it makes the scheme vulnerable to the attacks like noising.

Those algorithms stated previously [9]–[24] are carried out in the domain of tensor wavelet. In general, 2-D tensor wavelet filter banks are simply the tensor product of 1-D wavelet filter banks [26]. Although 1-D wavelet filter banks are proved to be compact supported, its tensor product can reveal the singularities in the three directions (i.e., horizontal, vertical, and diagonal) only [27]. In fact, a natural image contains the singularities in all directions. Tensor wavelets are unable to reveal them. Consequently, tensor wavelet filter banks cannot meet the watermarking requirements as follows [28], [29].

- Significant coefficients: considering the capacity of a watermarking scheme, the number of wavelet coefficients with large absolute values (i.e., significant coefficients) is of great importance [12], [13], [30].
- Invariances toward attacks: as watermarked images may encounter different kinds of distortions, the invariant property of wavelet transform, e.g., rotation invariance and scaling invariance, are quite meaningful [31].
- Abilities in revealing singularities: imperceptivity is an important requirement of a watermarking scheme. Considering the characteristics of HVS, singulary areas like edges and textural areas are suitable for watermark embedding. Thus, wavelet filter banks capable of capturing singularities are always desirable [32].

Further, according to [28], tensor wavelets suffer from the four shortcomings: 1) oscillations, 2) shift variance, 3) aliasing, and 4) lack of directionality.

In contrast, following the seminal work of Jelena *Kovačević*, nontensor product wavelets featuring revealing the singularities in all directions have been received much attention in the literature. In general, the high-frequency subbands of nontensor product wavelet transform can reveal more features than that of commonly used tensor wavelet one. Actually, the discrete nontensor product wavelet transform (DNWT) [33] has been used widely in the past decade. Nevertheless, the nontensor product wavelets within the framework of DNWT are problem-oriented. In this paper, we construct the new nontensor product wavelets for watermarking with linear phase that is constructed from the special symmetric matrices. This method provides a general way to construct wavelets. Actually, the proposed nontensor product wavelet filter banks are a general method for image processing and representation. It can be applied to image retrieval [34], [35], face recognition [36], [37], image quality assessment [38], and object categorization [39]. Tensor wavelets could be regarded as a special case of it by taking some specific parameters (see Section II-C for an example). With these new wavelets, more singularities can be utilized to embed watermark than that of discrete tensor wavelet transform (DWT). Moreover, the imperceptibility and robustness requirements of watermarking are fulfilled and optimized. Based upon the newly constructed nontensor product wavelet banks, we propose a watermarking scheme based upon significant differences in DNWT (SD-DNWT). In our previous work [40], we have partially exploited the new wavelet filter banks. However, [40] is a nonblind watermarking, in which the original image is need for watermarking extraction. In contrast, the proposed SD-DNWT watermarking is a blind watermarking. Experiments have shown that the performance of SD-DNWT watermarking outperforms the existing ones in tensor wavelet domain.

The rest of this paper is organized as follows. In Section II, the construction of new nontensor product wavelet filter banks is presented. Also, some examples and experimental results are shown. The detailed watermarking scheme is given in Section III. In Section IV, experiments are conducted to compare SD-DNWT with the existing ones. Finally, we draw a conclusion in Section V.

II. Construction of Nontensor Wavelet Filter Banks

A. Wavelet Construction Survey

The signal can be recovered from these subsampled signals by cancelling the aliasing terms with a particular class of filters called conjugate mirror filters (CMF) [41]. Design of the filter bank is still an active research topic in both signal and image processing. The sufficient and necessary conditions for decomposing a signal in subsampled components with a filtering scheme, and recovering the same signal with an inverse transform, were established in [42], [43].

Filter banks are closely associated with wavelets. The multiresolution theory shows that conjugate mirror filters and orthonormal wavelet basis of $L^2(R^d)$ are intimately linked. In fact, continuous-time wavelet basis can be obtained by the iterated filter banks, and filter banks can be considered as a discrete wavelet transform. The equivalence between the continuous time wavelet theory and discrete filter banks leads to a new fruitful interface between digital signal processing and harmonic analysis.

Multiresolution analysis (MRA) theory provides a natural framework for understanding wavelets and filter banks. According to MRA, refinable functions (scaling functions) and wavelets are completely determined by a low-pass filter and high-pass filters, respectively. In subband code schemes, a low-pass filter and high-pass filters are used, respectively, as analysis filter and synthesis filters which form perfect reconstruction filter banks. Daubechies [44] designed univariate two-channel perfect reconstruction filter banks having finite impulse response (FIR) corresponding to a univariate orthonormal wavelet having a compact support and vanishing moments. It is well known that there does not exist an orthonormal symmetric wavelet with a compact support in the univariate dyadic dilation case. That is, two-channel perfect reconstruction FIR banks having a linear phase are not available in the univariate case. Historically, this led to an intense interest in univariate multichannel, high-dimensional and vector-valued filter banks which correspond to M-band wavelets, multivariate wavelets and multiwavelets, respectively.

This paper concentrates on the multivariate filter banks [43]. Indeed, the study of the 2-D case is crucial for digital image processing. A commonly used method builds multivariate filter banks by the tensor products of univariate filters. This construction of filter banks focuses excessively on the coordinate direction. Therefore, nontensor product approaches for construction of multivariate filter banks or wavelets are desirable. Much interest has been given to the study of nontensor product wavelets in $L^2(R^d)$ [33], [45], [46] as well as to multiwavelets and corresponding vector-valued filter banks [47], [48].

However, it is not easy to design multivariate filter banks. At present, no general method is available for designing multivariate filter banks and vector-valued filter banks. There are two fundamental difficulties that one encounters in the design of the low-pass filters and high-pass filters which are used for the construction of refinable functions and wavelets, respectively. The first challenge lies in finding trigonometric polynomials that satisfy the perfect reconstruction condition, and the second is met when we extend a block unit vector of trigonometric polynomials to a unitary matrix. Most of the current studies in multivariate wavelets are given to a dilation matrix with the determinant two [33], [43]. In this case, only one high-pass filter is needed to be constructed and the matrix extension is the same as the univariate two-channel case [45].

Often, one seeks filter banks leading to smooth wavelets. However, in the application of filter banks to watermarking, experiments show that "smooth" filter banks are not suitable because images are not always smooth. Here, we describe a general construction of bivariate nontensor product wavelet filter banks with linear phase by using special symmetric matrices. The family of filter banks given in this paper is suitable in this context although it is difficult to achieve smoothness. These filter banks have a matrix factorization. It could reveal more singularities of image. This makes it more suitable for watermarking to optimize its performance in terms of imperceptibility and robustness.

B. Construction of Nontensor Wavelet Filter Banks

In this subsection, we describe a general construction of nontensor bivariate wavelet filter banks with a linear phase.

To construct two channel filter banks suitable for revealing image singularities at the whole orientations, we consider a special kind of symmetric orthogonal matrix of order 4

$$B = S \begin{pmatrix} Z_1 & 0 \\ 0 & Z_2 \end{pmatrix} S^T \tag{1}$$

where

$$S = \begin{pmatrix} 1 & 0 & 0 & -1 \\ 0 & 1 & -1 & 0 \\ 0 & 1 & 1 & 0 \\ 1 & 0 & 0 & 1 \end{pmatrix}$$

and Z_1 and Z_2 both of order 2×2 are orthogonal matrices. It is easily found that orthogonal matrices B has the following form:

$$B = \frac{1}{2} S \begin{pmatrix} a & b & 0 & 0 \\ c & d & 0 & 0 \\ 0 & 0 & e & f \\ 0 & 0 & g & h \end{pmatrix} S^T \tag{2}$$

with real numbers a, b, c, d, e, f, g, h satisfying

$$a^2 + b^2 = c^2 + d^2 = 1, \quad ac + bd = 0$$
$$e^2 + f^2 = g^2 + h^2 = 1, \quad eg + fh = 0.$$

The parametrization solutions of the previously shown equations for these real numbers are $a = d = \cos\alpha$, $b = -\sin\alpha$, $c = \sin\alpha$, $e = h = \cos\beta$, $f = -\sin\beta$ and $g = \sin\beta$, for any real numbers α and β. Therefore, any of the previously shown special symmetric orthogonal matrix B has the more simple parametrization representation, i.e.,

$$B = \frac{1}{2} S \begin{pmatrix} \cos\alpha & -\sin\alpha & 0 & 0 \\ \sin\alpha & \cos\alpha & 0 & 0 \\ 0 & 0 & \cos\beta & -\sin\beta \\ 0 & 0 & \sin\beta & \cos\beta \end{pmatrix} S^T \tag{3}$$

for some real number α and β.

It can be written as

$$B_{(\alpha,\beta)} := \frac{1}{2}\begin{pmatrix} z_1+z_3 & -z_2+z_4 & -z_2-z_4 & z_1-z_3 \\ z_2-z_4 & z_1+z_3 & z_1-z_3 & z_2+z_4 \\ z_2+z_4 & z_1-z_3 & z_1+z_3 & z_2-z_4 \\ z_1-z_3 & -z_2-z_4 & -z_2+z_4 & z_1+z_3 \end{pmatrix} \tag{4}$$

where $z_1=\cos\alpha$, $z_2=\sin\alpha$, $z_3=\cos\beta$, $z_4=\sin\beta$.

Letting $u=e^{-i\xi}$, $v=e^{-i\eta}$, we define a bivariate trigonometric polynomials as follows:

$$h_0(u,v)=\sum_{j\in Z}\sum_{k\in Z} c_{j,k}u^j v^k, \qquad (u,v)\in \partial D\times\partial D$$

where $D=\{z:|z|\le 1\}$, $\partial D=\{z:|z|=1\}$. Its polyphase factors are the bivariate trigonometric polynomials $h_{0,l}$ defined for $l=$0, 1, 2, and 3 as

$$\begin{aligned} h_{0,0}(u,v)&=\sum_{j\in Z}\sum_{k\in Z} c_{2j,2k}u^j v^k \\ h_{0,1}(u,v)&=\sum_{j\in Z}\sum_{k\in Z} c_{2j+1,2k}u^j v^k \\ h_{0,2}(u,v)&=\sum_{j\in Z}\sum_{k\in Z} c_{2j,2k+1}u^j v^k \\ h_{0,3}(u,v)&=\sum_{j\in Z}\sum_{k\in Z} c_{2j+1,2k+1}u^j v^k. \end{aligned}$$

Reversing the process, we can construct the bivariate trigonometric polynomials h_0 from its polyphase factors $h_{0,l}$, $j=$0, 1, 2, and 3 by the formula

$$\begin{aligned} h_0(u,v)=h_{0,0}(u^2,v^2)+uh_{0,1}(u^2,v^2) \\ +vh_{0,2}(u^2,v^2)+uvh_{0,3}(u^2,v^2). \end{aligned}$$

The construction of bivariate compactly supported orthonormal multiwavelets using multiresolution analysis (MRA) is equivalent to the design of orthogonal FIR and QMF filter banks, which leads to the following two problems:

1) find the low-pass filter $h_0(u,v)$ satisfying the orthogonal condition

$$|h_0(u,v)|^2+|h_0(-u,v)|^2+|h_0(u,-v)|^2+|h_0(-u,-v)|^2=1;$$

2) find three high-pass filters h_1,h_2,h_3 such that the matrix

$$\begin{pmatrix} h_0(u,v) & h_0(-u,v) & h_0(u,-v) & h_0(-u,-v) \\ h_1(u,v) & h_1(-u,v) & h_1(u,-v) & h_1(-u,-v) \\ h_2(u,v) & h_2(-u,v) & h_2(u,-v) & h_2(-u,-v) \\ h_3(u,v) & h_3(-u,v) & h_3(u,-v) & h_3(-u,-v) \end{pmatrix}$$

is unitary. Given the orthogonal filter banks h_l, $l=$0, 1, 2, 3 at hand, one can use Pyramid algorithm [49] to decompose and reconstruct the signal (i.e., image). It will benefit us from the point view of polyphase to understand the conditions in Problem 1) and 2).

a) Find a bivariate trigonometric polynomials h_0 such that its polyphase factors $h_{0,l}$, $l=$0, 1, 2, 3, satisfy

$$M_0(u,v)M_0(u,v)^*=\frac{1}{4}I_r, \qquad (u,v)\in\partial D\times\partial D \tag{5}$$

where M_0 is a 1×4 matrix defined by

$$M_0(u,v):=(h_{0,0}(u,v),h_{0,1}(u,v),h_{0,2}(u,v),h_{0,3}(u,v))$$

and I_r is the identity matrix of order r.

b) Find three bivariate trigonometric polynomials h_1,h_2,h_3 such that the 4×4 matrix composed of their polyphase factors given by

$$M(u,v):=\begin{pmatrix} h_{0,0}(u,v) & h_{0,1}(u,v) & h_{0,2}(u,v) & h_{0,3}(u,v) \\ h_{1,0}(u,v) & h_{1,1}(u,v) & h_{1,2}(u,v) & h_{1,3}(u,v) \\ h_{2,0}(u,v) & h_{2,1}(u,v) & h_{2,2}(u,v) & h_{2,3}(u,v) \\ h_{3,0}(u,v) & h_{3,1}(u,v) & h_{3,2}(u,v) & h_{3,3}(u,v) \end{pmatrix} \tag{6}$$

has the property that $2M(u,v)$ is a unitary matrix. Here, for fixed $j\in\{1,2,3\}$, $h_{j,l}$, with $l=$0, 1, 2, 3 denotes the polyphase factors of h_j.

Both of Problems 1) and 2) [equivalently a) and b)] are nonlinear and, essentially, quadratic algebraic equations with multiple variables. There is no general solution for such a problem presently. Now we will offer a class of solutions of Problem 1) and 2) starting from special symmetric matrix.

Let

$$\begin{aligned} E_0&=(1,1,1,1)^T, \qquad E_1=(1,-1,1,-1) \\ E_2&=(1,1,-1,-1)^T, \qquad E_3=(1,-1,-1,1) \end{aligned} \tag{7}$$

and denote the matrix of trigonometric polynomial by $T(u,v)$ with

$$T(u,v)=\begin{pmatrix} 1 & 0 & 0 & 0 \\ 0 & u & 0 & 0 \\ 0 & 0 & v & 0 \\ 0 & 0 & 0 & uv \end{pmatrix}, \qquad (u,v)\in\partial D\times\partial D. \tag{8}$$

For any fixed positive integer N, we arbitrarily choose real number pairs (α_k,β_k), $k=1,2,\ldots,N$ (for $k\ne j$, (α_k,β_k) may equal to (α_j,β_j)). The low-pass filter $h_0(u,v)$ is defined as follows:

$$h_0(u,v)=\frac{1}{4}(1,u,v,uv)\left(\prod_{k=1}^{N} B_{(\alpha_k,\beta_k)}T(u^2,v^2)B^T_{(\alpha_k,\beta_k)}\right)E_0 \qquad (u,v)\in\partial D\times\partial D \tag{9}$$

where $B_{(\alpha_k,\beta_k)}$ is a special symmetric orthogonal matrix defined in (4). It is easy to see that $h(0,0)=1$, which means that h_0 is a low-pass filter. We will show that h_0 satisfies the condition (5) and has the uniform linear phase. Here we say h_0 has a uniform linear phase if there exists two integers μ_1 and μ_2 such that

$$\overline{h_0(u,v)}=u^{\mu_1}v^{\mu_2}h_0(u,v). \tag{10}$$

Next, we will construct the three high-pass filters h_j, $j=$1, 2, 3 with respect to the previously shown low-pass filter $h_0(u,v)$ and show that they form perfect reconstructional filter banks. Let

$$h_j(u,v)=\frac{1}{4}(1,u,v,uv)\left(\prod_{k=1}^{N} B_{(\alpha_k,\beta_k)}T(u^2,v^2)B^T_{(\alpha_k,\beta_k)}\right)E_j \qquad j=1,2,3 \tag{11}$$

with E_j defined in (7). It is easy to find that $h_j(0,0)=0$, $j=1$, 2, 3. That is, h_j, $j=1$, 2, 3 are the high-pass filters.

Theorem: The low-pass filter h_0 defined in (9) has a linear phase and $\{h_0,h_1,h_2,h_3\}$ defined in (9) and (11) form the perfect reconstructional FIR orthogonal filter banks.

Proof: To prove $\{h_0,h_1,h_2,h_3\}$ satisfies the perfect reconstructional conditions, it is sufficient to show that the polyphase matrix $M(u,v)$ generated from h_j, $j=0$, 1, 2, 3 satisfies

$$M(u,v)M^*(u,v)=\frac{1}{4}I_4.$$

It follows from (9) and (11) that the polyphase matrix $M(u,v)$ is of the form

$$M^T(u,v)=\frac{1}{4}\left(\prod_{k=1}^{N}B_{(\alpha_k,\beta_k)}T(u^2,v^2)B^T_{(\alpha_k,\beta_k)}\right)\times(E_0,E_1,E_2,E_3).$$

Since all the matrices $B_{(\alpha_j,\beta_j)}$, $j=1,2,\ldots,$ N, and $T(u,v)$ are unitary and the matrix $(1/2)(E_0,E_1,E_2,E_3)$ is orthogonal, we conclude that the matrix $2M(u,v)$ is unitary as well.

Now we turn to prove h_0 has a uniform linear phase. By the definition of h_0, we have

$$\overline{h_0(u,v)}=\frac{1}{4}(1,u,v,uv)\times\left(\prod_{k=1}^{N}B_{(\alpha_k,\beta_k)}T(u^{-2},v^{-2})B^T_{(\alpha_k,\beta_k)}\right)E_0.$$

By using the equations

$$u^2v^2T(u^{-2},v^{-2})=H_4T(u^2,v^2)H_4$$

and

$$uv(1,u,v,uv)=(1,u^{-1},v^{-1},u^{-1}v^{-1})H_4$$

where

$$H_4=\begin{pmatrix}0&0&0&1\\0&0&1&0\\0&1&0&0\\1&0&0&0\end{pmatrix}.$$

We conclude that

$$\overline{h_0(u,v)}=\frac{1}{4}u^{2N+1}v^{2N+1}(1,u^{-1},v^{-1},u^{-1}v^{-1})H_4*\left(\prod_{k=1}^{N}B_{(\alpha_k,\beta_k)}H_4T(u^2,v^2)H_4B^T_{(\alpha_k,\beta_k)}\right)E_0$$

from which it follows that:

$$\overline{h_0(u,v)}=\frac{1}{4}u^{2N+1}v^{2N+1}(1,u^{-1},v^{-1},u^{-1}v^{-1})*\left(\prod_{k=1}^{N}H_4B_{(\alpha_k,\beta_k)}H_4T(u^2,v^2)H_4B^T_{(\alpha_k,\beta_k)}H_4\right)H_4E_0.$$

Combining this equation with the facts

$$H_4B_{(\alpha_k,\beta_k)}H_4=B_{(\alpha_k,\beta_k)},\quad H_4B^T_{(\alpha_k,\beta_k)}H_4=B^T_{(\alpha_k,\beta_k)}$$
$$H_4E_0=E_0$$

we conclude that

$$\overline{h_0(u,v)}=\frac{1}{4}u^{2N+1}v^{2N+1}h_0(u,v).$$

The proof of this theorem is completed. □

These filter banks have a matrix factorization and can be used in image. In signal processing, a linear phase is a central property of filters. Under this condition, if an input signal has energy confined to the pass-band of the filter, the out signal is approximately equal to the input. It is well known that, in the univariate case, the only two channel CMF and FIR filter banks with a linear phase are the Haar filters.

C. Examples of Nontensor Bivariate Wavelet Filter

Next we will give several concrete examples of filter banks obtained by the proposed method.

Example 1: Let $\alpha=0$, $\beta=0$, by (4), we can lead to the important special symmetric orthogonal matrix

$$B_{(0,0)}=\begin{pmatrix}1&0&0&0\\0&1&0&0\\0&0&1&0\\0&0&0&1\end{pmatrix}.$$

Further, setting $N=1$, the previous matrix $B_{(0,0)}$ leads to the following filter banks:

$$\begin{cases}h_0(u,v)=\frac{1}{4}(1+u^3+v^3+u^3v^3)\\h_1(u,v)=\frac{1}{4}(1-u^3+v^3-u^3v^3)\\h_2(u,v)=\frac{1}{4}(1+u^3-v^3-u^3v^3)\\h_3(u,v)=\frac{1}{4}(1-u^3-v^3+u^3v^3).\end{cases}$$

The filter banks can be represented in matrix form as follows:

$$h_0=\begin{pmatrix}0.25&0&0&0.25\\0&0&0&0\\0&0&0&0\\0.25&0&0&0.25\end{pmatrix}$$
$$h_1=\begin{pmatrix}0.25&0&0&-0.25\\0&0&0&0\\0&0&0&0\\0.25&0&0&-0.25\end{pmatrix}\qquad(12)$$
$$h_2=\begin{pmatrix}0.25&0&0&0.25\\0&0&0&0\\0&0&0&0\\-0.25&0&0&-0.25\end{pmatrix}$$
$$h_3=\begin{pmatrix}0.25&0&0&-0.25\\0&0&0&0\\0&0&0&0\\-0.25&0&0&0.25\end{pmatrix}.\qquad(13)$$

In fact, these filters are tensors. They are tensor products of two 1-D filter $h=(0.5,0,0,0.5)$ and $g=(0.5,0,0,-0.5)$. In other words, a tensor filter can be generated by taking some special α,

β. Thus, the tensor filter bank can be regarded as a special case of the proposed nontensor filter banks.

Example 1 is a simple and special implementation of our method. A more complicated and general example are shown as follows.

Example 2: According to (9) and (11), the filter size grows with N (i.e., filter size $= 2(N+1)\times 2(N+1)$). This means that the filter banks could be constructed adaptively to the image size by changing N. Meanwhile, N pairs of parameters (α_k, β_k), $k = 1, \ldots, N$, could be selected to reveal singularities in various directions. Let $N = 2$, $(\alpha_1 = \pi/3, \beta_1 = \pi/4)$, $(\alpha_2 = 0.75, \beta_2 = 0.95)$, respectively, from (4), (9), and (11). We will have the nontensor filter banks shown in (14)–(17) at the bottom of the page.

The size of nontensor product wavelet filter grows with parameter N. The size of each filter is $(2N+2)\times(2N+2)$. Fig. 1 shows a nontensor product wavelet filter banks with $N = 12$, in which the size of these filters is 26×26.

Thus far, we have presented a method for constructing nontensor wavelet filter banks.

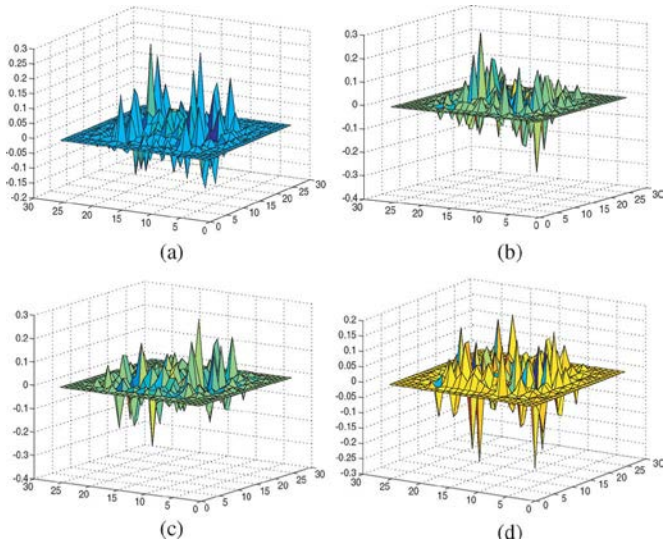

Fig. 1. Nontensor product wavelet filter bank with $N = 12$.

D. Evaluation of Nontensor Filter Banks Based Upon Experimental Realization

In this subsection, we will show the improvement of revealing singularities achieved by nontensor product wavelet filter banks in contract with tensor wavelets. For nontensor product wavelet construction, parameters N, α and β were set at 1, 0.78, and 1.05, respectively, by a rule of thumb. Meanwhile, $db4$ wavelet filter banks were selected as a representative of tensor wavelet banks.

Firstly, we utilized the newly constructed wavelet filter banks to decompose image "window"(see Fig. 2). It contains various directional singularities which cannot be revealed by conventional wavelet banks (see Fig. 4). The result is shown in Fig. 5. It can be seen that much more singularities are revealed in the three subimages.

$$h_0 = \begin{pmatrix} 0.2071 & 0.0273 & 0.0081 & -0.0485 & -0.0010 & 0.0073 \\ 0.2699 & -0.0355 & 0.0106 & 0.0632 & -0.0013 & -0.0096 \\ 0.0184 & 0.0024 & -0.0025 & -0.0047 & 0.0017 & -0.0131 \\ -0.0131 & 0.0017 & -0.0047 & -0.0025 & 0.0024 & 0.0184 \\ -0.0096 & -0.0013 & 0.0632 & 0.0106 & -0.0355 & 0.2699 \\ 0.0073 & -0.0010 & -0.0485 & 0.0081 & 0.0273 & 0.2071 \end{pmatrix} \tag{14}$$

$$h_1 = \begin{pmatrix} 0.2045 & 0.0269 & 0.0143 & -0.0470 & -0.0045 & 0.0340 \\ 0.2665 & -0.0351 & 0.0187 & 0.0613 & -0.0058 & -0.0443 \\ 0.0154 & 0.0020 & 0.0044 & -0.0031 & -0.0022 & 0.0165 \\ -0.0165 & 0.0022 & 0.0031 & -0.0044 & -0.0020 & -0.0154 \\ 0.0443 & 0.0058 & -0.0613 & -0.0187 & 0.0351 & -0.2665 \\ -0.0340 & 0.0045 & 0.0470 & -0.0143 & -0.0269 & -0.2045 \end{pmatrix} \tag{15}$$

$$h_2 = \begin{pmatrix} -0.0340 & -0.0045 & 0.0470 & 0.0143 & -0.0269 & 0.2045 \\ -0.0443 & 0.0058 & 0.0613 & -0.0187 & -0.0351 & -0.2665 \\ -0.0165 & -0.0022 & 0.0031 & 0.0044 & -0.0020 & 0.0154 \\ -0.0154 & 0.0020 & -0.0044 & -0.0031 & 0.0022 & 0.0165 \\ 0.2665 & 0.0351 & 0.0187 & -0.0613 & -0.0058 & 0.0443 \\ -0.2045 & 0.0269 & -0.0143 & -0.0470 & 0.0045 & 0.0340 \end{pmatrix} \tag{16}$$

$$h_3 = \begin{pmatrix} 0.0073 & 0.0010 & -0.0485 & -0.0081 & 0.0273 & -0.2071 \\ 0.0096 & -0.0013 & -0.0632 & 0.0106 & 0.0355 & 0.2699 \\ -0.0131 & -0.0017 & -0.0047 & 0.0025 & 0.0024 & -0.0184 \\ -0.0184 & 0.0024 & 0.0025 & -0.0047 & -0.0017 & -0.0131 \\ 0.2699 & 0.0355 & 0.0106 & -0.0632 & -0.0013 & 0.0096 \\ -0.2071 & 0.0273 & -0.0081 & -0.0485 & 0.0010 & 0.0073 \end{pmatrix} \tag{17}$$

Fig. 2. Original image "window."

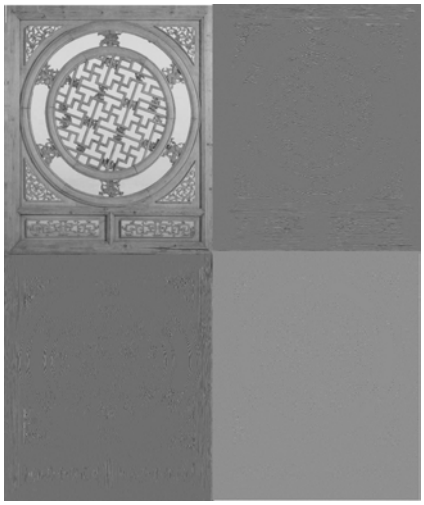

Fig. 3. "db4" wavelet decomposed the image of "window:" The upper left subimage is the approximation subimage. The upper right subimage reveals the singularities in the horizontal direction. The left bottom subimage reveals the singularities in the vertical direction. The right bottom subimage reveals the singularities in the diagonal direction. Singularities orienting at the other directions are unable to be revealed by the tensor wavelet.

Fig. 4. "Haar" wavelet decomposed the image of "window:" The upper left subimage is the approximation subimage. The upper right subimage reveals the singularities in the horizontal direction. The left bottom subimage reveals the singularities in the vertical direction. The right bottom subimage reveals the singularities in the diagonal direction. Singularities orienting at the other directions are unable to be revealed by the tensor wavelet.

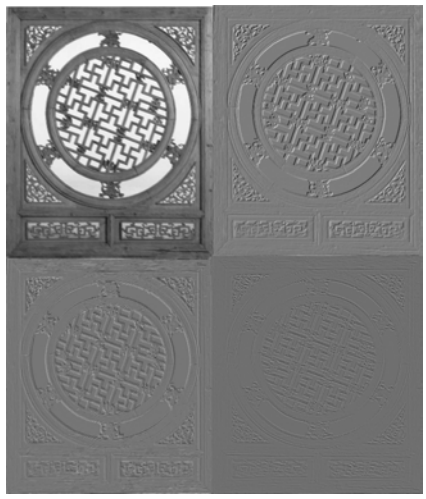

Fig. 5. Nontensor product wavelet decomposed the image of "window," in which much more singularities are revealed in subimages compared to Fig. 4.

The comparisons of the number of significant coefficients are shown from Fig. 6 to Fig. 9, where the vertical coordinate means the natural logarithms of the number of coefficients. It clearly shows that there are much more significant coefficients in nontensor product wavelet high frequency subbands than both "haar" and "db4" wavelets. Significant coefficients indicate the singularities of images. Larger number of significant coefficients means the higher ability in revealing image singularities.

Then we utilized the standard image "fishing boat" (see Fig. 10) for further analysis. Nontensor product wavelet transform and tensor wavelet transform were applied to "boat," respectively (see Fig. 11). In the high-frequency subimages of nontensor product wavelet decomposition, more features are revealed than that of tensor wavelet decomposition.

To make this difference more intuitively, we binarized the upper left high-frequency subimage of Fig. 11(a) and (b). Note that other subimages were also feasible. The positive coefficients were set at 1, while the negative coefficients were set at 0 (see Fig. 12). It could be observed clearly that singularities (e.g., edges) of the boat are apparent in Fig. 12(a), while its counterpart in Fig. 12(b) is almost unnoticable.

For the purpose of comparing nontensor product wavelet's ability in revealing singularities in various directions with tensor wavelet, we utilized the image "copper coins" (Fig. 13) which contains several apparent directional components. From Figs. 14 and 15, in the high-frequency subimages of nontensor product wavelet, more singularities in various directions were revealed. But in the subimages of tensor wavelet, only singularities in a single direction were revealed in each subimage.

In order to quantitatively analyze the ability in revealing singularities of nontensor product wavelet filter banks, we applied the DNWT and DWT to 10 images obtained from [50]. All these images were of size 512×512. We computed the

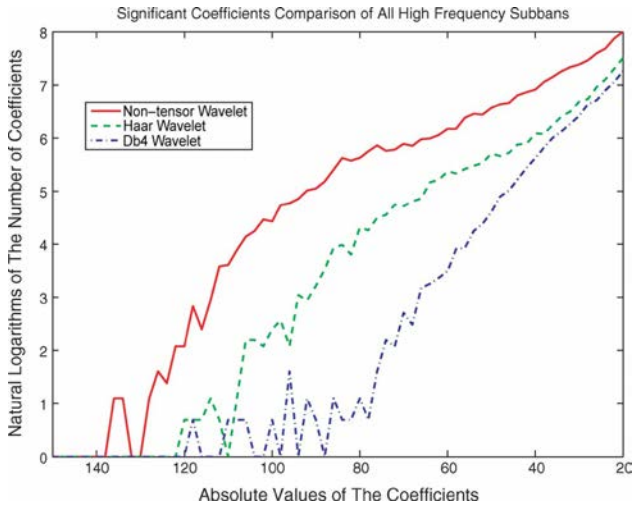

Fig. 6. Comparison of significant coefficients in all high frequency subbands.

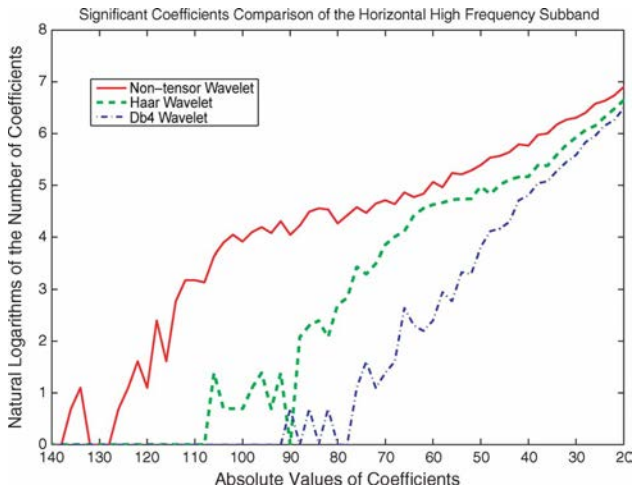

Fig. 7. Comparison of significant coefficients in horizonal high frequency subbands.

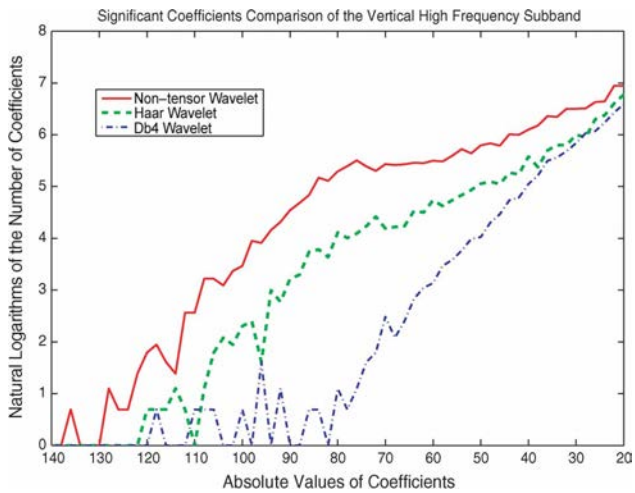

Fig. 8. Comparison of significant coefficients in vertical high frequency subbands.

absolute values of the upper right high-frequency subimages of the 10 images. There were in total $256 \times 256 \times 10 = 655,360$

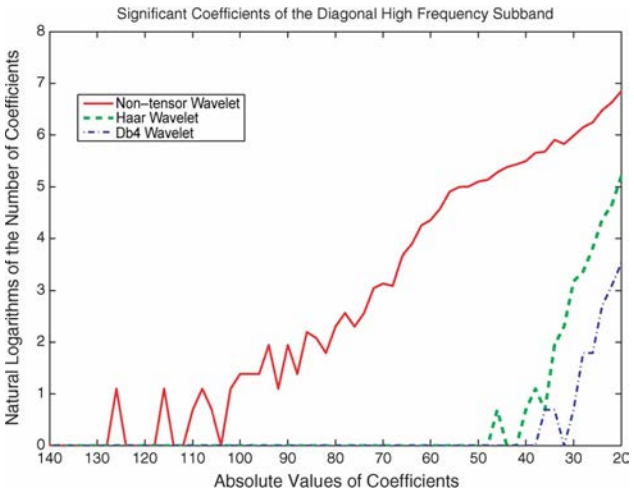

Fig. 9. Comparison of significant coefficients in diagonal high frequency subbands.

Fig. 10. Original image: "boat."

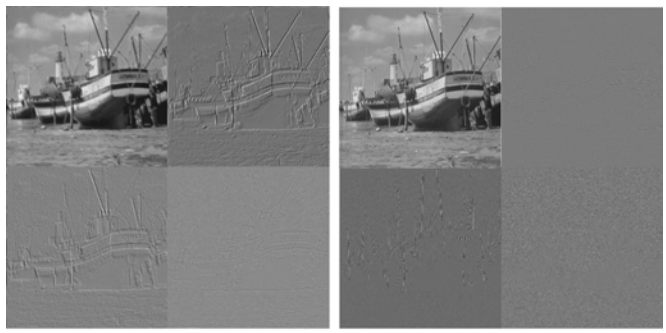

Fig. 11. Wavelet decomposition. (a) Subimages of DNWT. (b) Subimages of DWT $(db4)$.

elements for ten subimages. We analyzed the cumulative distribution function (CDF) of these values (see Fig. 16). From Fig. 16, 91.5% of "$db4$" wavelet coefficients were smaller than 15, while only 59% of nontensor product wavelet coefficients were smaller than 15. On the other hand, there were almost no coefficient greater than 60 in "$db4$" subimages, while more than

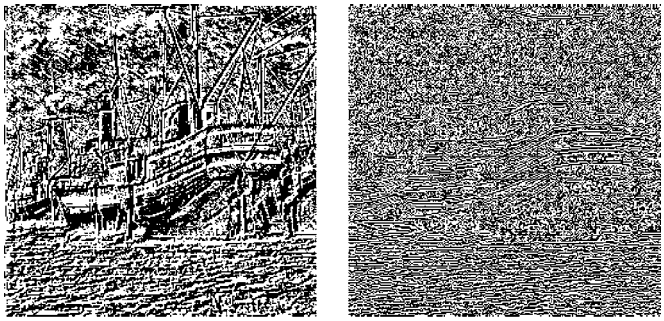

(a) (b)

Fig. 12. Binarized high frequent subimages. (a) Nontensor product wavelet with $\alpha = 0.78$, $\beta = 1.05$, and $N = 1$. (b) Tensor wavelet $(db4)$.

Fig. 13. Original image "copper coin."

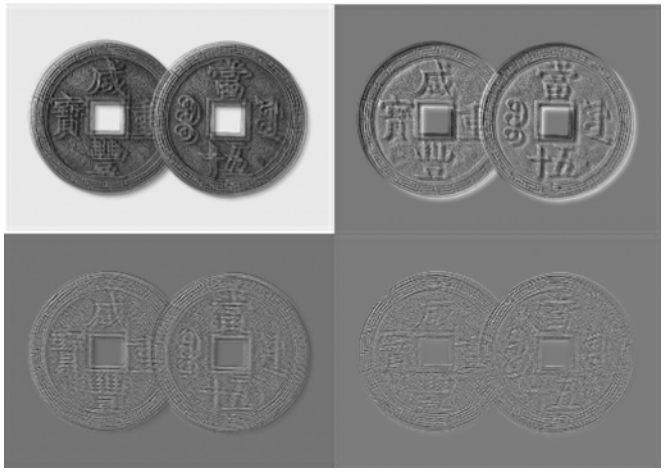

Fig. 14. Nontensor product wavelet subimages of "copper coin."

5% of nontensor product wavelet coefficients were larger than 60. Due to the high capacity of nontensor product wavelet filter banks in revealing singularities along the various directions, there are more significant coefficients in nontensor product wavelet high-frequency subimages. As significant coefficients are desirable in watermark embedding, it is naturally necessary to apply DNWT into watermarking algorithm design. Experimental results show that our algorithm outperforms the ones proposed in tensor wavelet domain.

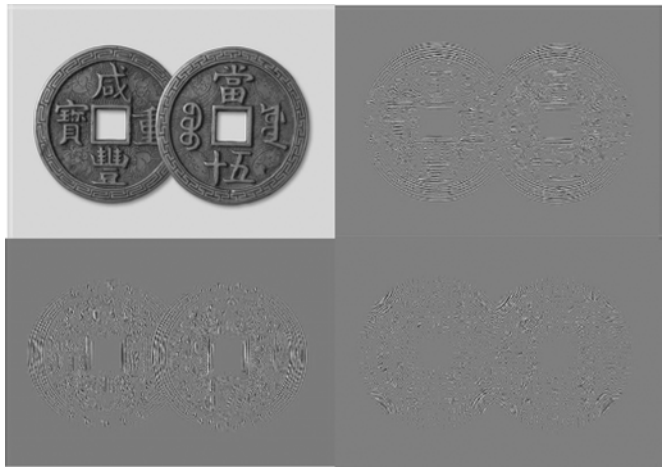

Fig. 15. Tensor wavelet subimages of "copper coin."

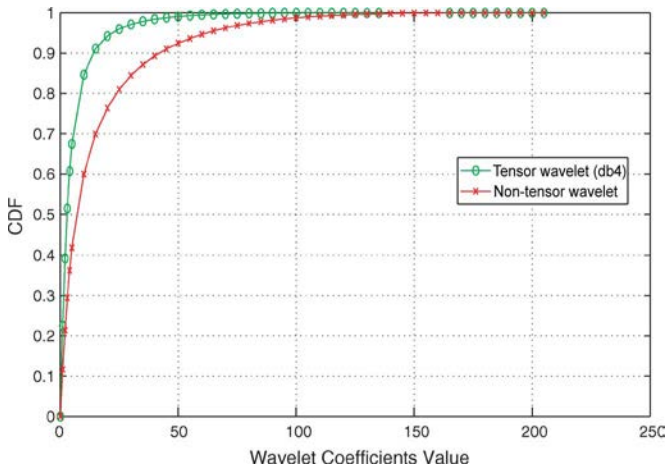

Fig. 16. CDF of "db4" and nontensor product wavelet coefficients based upon ten commonly used images.

From the previously shown analysis, we can find some desirable properties in watermarking. Compared to the traditional tensor wavelets, nontensor product wavelet filter banks have the properties suitable for watermarking:

1) larger number of significant coefficients (see Fig. 6, Fig. 7, Fig. 8, Fig. 9, and Fig. 16);
2) higher ability in revealing image singularities in various directions (see Fig. 11 and Fig. 12).

These properties, sometimes implicitly, meet the requirements arisen in Section I. It is imperative to make good use of these desirable properties in watermarking scheme design.

III. Watermarking Based Upon Nontensor Product Wavelet Filter Banks

In this section, after analyzing [21] and property of nontensor product wavelet filters banks, a modified significant difference watermarking algorithm is developed.

Original image is decomposed using 3-level wavelet transform. Every seven nonoverlap wavelet coefficients in subimage H_1^3 are grouped into a block. In each block, the largest and

second largest wavelet coefficients are called significant coefficients and the difference between them is so called significant difference. The average significant difference value is defined as

$$\xi = \frac{1}{N}\sum_{i=1}^{N}(C_i^m - C_i^s) \tag{18}$$

where N, C_i^m, and C_i^s are the number of watermark bits, the maximum wavelet and second maximum wavelet coefficient in each block, respectively, and $i(1 \le i \le N)$ is the index of block. The number of block is equal to the number of watermark bits.

In the ith block, if the watermark bit $W_i = 1$, we quantize C_i^m with threshold T as

$$C_i^m = \begin{cases} C_i^s + T, & \text{if } (C_i^m - C_i^s) < \text{maximum}(\xi, T) \\ C_i^m, & \text{if } (C_i^m - C_i^s \ge \text{maximum}(\xi, T). \end{cases} \tag{19}$$

Otherwise, if the watermark bit $W_i = 0$, C_i^m is quantized as

$$C_i^m = C_i^s. \tag{20}$$

By repeating these procedures, all watermark bits will be embedded. Concerning the extracting phase, the adaptive threshold is set at

$$T_a = \frac{1}{N \times \alpha}\sum_{j=1}^{N\times\alpha}\chi_j \tag{21}$$

where α is the scale parameter that determines the number of the significant differences which can be averaged. χ is the vector which contains all the significant differences in an ascending order.

Watermark extracting method is the inverse process of watermark embedding and rather straightforward. Watermark bits are extracted according to

$$Wi = \begin{cases} 1, & \text{if } (C_i^m - C_i^s) \ge T_a \\ 0, & \text{otherwise.} \end{cases} \tag{22}$$

This algorithm well exploits significant coefficients in wavelet domain. As we stated previously, significant coefficients in the high frequency wavelet subbands reveal the singularities which are suitable for watermark embedding. However, its performance at the same time might be undermined by inability in revealing singularities in various directions of tensor wavelet coefficients. It is well known that the existing wavelet subbands can only reveal singularities in the three directions (i.e., horizonal, vertical, and diagonal). Significant difference plays a key role of the algorithm. It directly determines the watermarking strength. Large significant difference can tolerate large coefficient modification, i.e., watermarking strength. As shown in Table I, significant differences in the nontensor product wavelet domain are obviously larger than its counterpart in tensor wavelet domain.

Based upon the previous analysis, we propose a significant difference watermarking scheme in nontensor product wavelet domain. Different from [21], all the three high frequency subbands are used to embed watermarks. This implies that we can embed more watermark bits and simultaneously achieve good imperceptibility and robustness. This is benefit from nontensor product wavelet filter banks' superior ability in revealing image singularities along all direction rather than the three directions only revealed by a traditional tensor product wavelet. For example, paper [21] utilizes the horizonal high frequency subband H_1^3 only. Since image singularities may orient at various directions, only the horizonal high frequency subband cannot optimally meet the imperceptibility requirement. It misses many useful singularities. In contrast, the use of nontensor product wavelet filter banks can make the algorithm more flexible. More subbands and more coefficients can be used to embed watermarks.

TABLE I
COMPARISONS OF SIGNIFICANT DIFFERENCES IN TENSOR WAVELET AND NONTENSOR PRODUCT WAVELET DOMAIN, WHERE THE BLOCK SIZE IS 7

	trees	airplane	bridge	girl	peppers
"Db4"	49.8	32.2	42.8	20.9	29.2
"Non-tensor"	101.8	75.4	84.4	67.3	86.6
	house	earth	elaine	lena	baboon
	31.2	37.5	24.3	26.0	39.7
	73.7	82.8	104.3	94.8	79.0

The proposed algorithm can be summarized as follows.

Step 1) ***Preprocessing of Watermarks***
The 2-D binary watermark $W = \{w(i,j), i,j \in N, 1 \le i \le m, 1 \le j \le n\}$ is reshaped into 1-D vector $S = \{s(l), l \in N, 1 \le l \le m \times n\}$. We then encrypt and scramble it by a private key K_1 for security and the relativity reduction of cropping.

Step 2) ***Nontensor Product Wavelet Decomposition***
Apply 3 level nontensor product wavelet decomposition to the original image using our wavelet filter banks constructed in Section II. As the size of filter banks grows with N, parameter N should be selected according to the size of the original image.

Step 3) ***Preprocessing of Blocks***
Every seven nonoverlap wavelet coefficients in the high frequency subbands are grouped into a block. The blocks are randomly shuffled by another private key K_2.

Step 4) ***Computation of Average Significant Differences***
Compute the average significant differences for all blocks using (18).

Step 5) ***Watermark Embedding***
Search C_i^m and C_i^s of each block. Compute their difference (i.e., significant difference). If the watermark bit to be embedded is 1, quantize C_i^m according to (19). Otherwise, quantize C_i^m according to (20) if the watermark bit to be embedded is 0.

Step 6) ***Inverse Nontensor Product Wavelet Transform***
Reshuffle all the blocks by K_2. Apply inverse nontensor product wavelet transform to the modified coefficients. Then, the watermarked image is obtained.

Figs. 17 and 18 show a general frame of the embedding scheme and the way of coefficients modification, respectively.

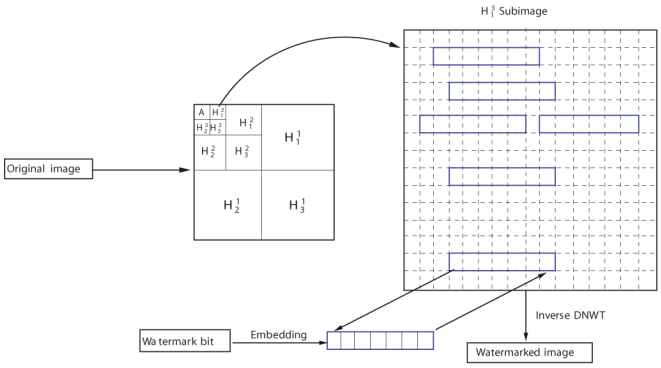

Fig. 17. Process of watermark embedding.

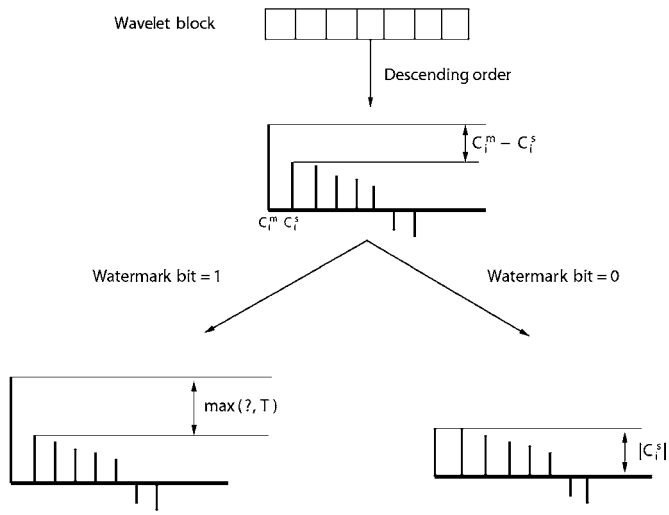

Fig. 18. Fashion of nontensor product wavelet coefficient modifying.

Watermark extracting is the inverse procedure of watermark embedding. The steps of watermark extraction are listed as follows:

Step 1) Apply 3 level nontensor product wavelet decomposition to the watermarked image using our wavelet filter banks constructed in Section II.

Step 2) Every seven nonoverlap coefficients in all high frequency subimages are grouped into a block. These blocks are shuffled according to the private key K_2.

Step 3) Compute the extracting threshold T_a according to (21).

Step 4) In each block, the watermark is extracted according to (22).

Step 5) These extracted watermark bits are reshuffled by private key K_1. Then, we obtain the watermark pattern.

IV. Experiments and Evaluations

This section investigated on the performance of the proposed algorithm. Several distortion including unintentional attacks like JPEG compression, filtering and noising as well as the intentional attacks like cropping, rotation were applied in the watermarked images. The Stirmark benchmark [50] and PhotoImpact 13 software [51] were utilized to attack the images. The parameters α, β and N for constructing nontensor product wavelet banks were 0.78, 1.05, and 1, respectively.

Fig. 19. Original image and original watermark pattern.

Fig. 20. Watermarked image with PSNR $=$ 42 db and extracted watermark with NC $=$ 1.

From Fig. 19 and 20, we can see that there is no visible degradation in the watermarked image (PSNR $= 42$ db) and the watermark could be extracted with $NC = 1$, where the normalization correlation (NC), defined as

$$\mathrm{NC} = \frac{\sum_i^j W(i,j) * W'(i,j)}{\sqrt{\sum_i^j W(i,j)^2 * \sum_i^j W'(i,j)^2}} \tag{23}$$

is used as a criterion for evaluating watermarking performance, where $W(i,j)$ is the original watermark, and $W'(i,j)$ is the extracted watermark.

Regarding the JPEG compression attacks, we tested the performances of the 10 standard images listed in Table I, where the curve of the NC value versus JPEG Quality Factor (QF) is shown in Fig. 22. NC values are the average normalized correlation values of the 10 images. Fig. 21 shows the watermarked image "boat" after JPEG compression (QF $= 60\%$) and extracted watermark. From Fig. 22, we can see that the watermark could be kept in a quite low JPEG Quality Factor.

As for the robustness against noising, the distorted watermarked images with different variances were tested. To show watermarking's superiority in nontensor product wavelet domain against noising attacks, we also tested the watermarking

Fig. 21. Watermarked image after JPEG compression (QF = 35%) with PSNR = 29.5 db and extracted watermark with NC = 0.7532.

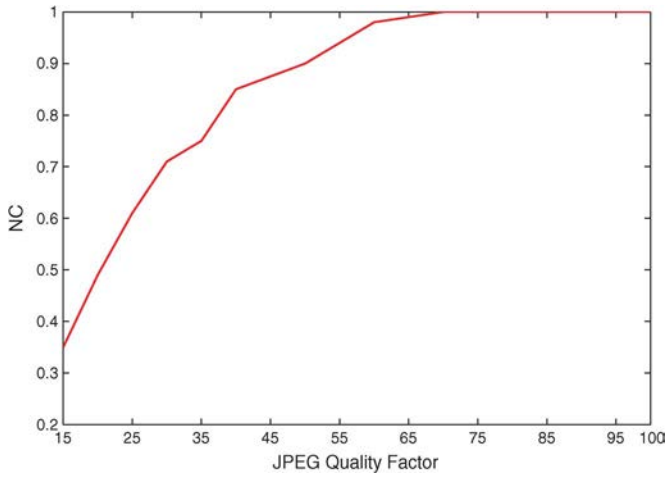

Fig. 22. Curve of the extracted watermark NC value versus JPEG Quality Factor

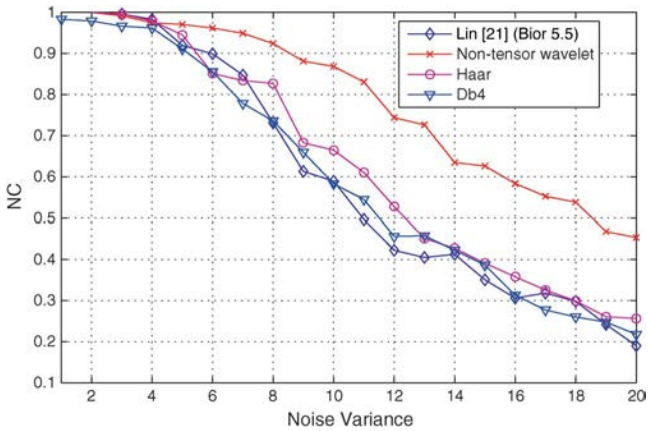

Fig. 23. Extracted watermark NC value versus noise variances curves.

algorithms in tensor wavelet domain. The NC values are the average value of the ten standard image as shown in Table I. The results are shown in Fig. 23.

In addition, the cropping and rotation were also applied to the watermarked images to test the proposed algorithm's robustness. For cropping, watermark should cover the entire image from a cropped image, i.e., some parts of the image are cut away.

TABLE II
PERFORMANCE OF PROPOSED WATERMARKING ALGORITHM AGAINST ATTACKS

	Cropping (75%)	Rotation (0.25)
non-tensor product wavelet	0.5533	0.7900
Lin [21] (Bior 5.5)	0.4441	0.6052
Db4	0.5720	0.5433
Haar	0.3345	0.5240

TABLE III
PERFORMANCE COMPARISON BETWEEN OUR METHOD (SD-DNWT) AND WANG'S [20]

Image operations	JPEG (QF=90%)	JPEG (QF=50%)	JPEG (QF=30%)
Our method	1.00	0.95	0.77
Wang's [20]	1.00	0.57	0.15
	Rotation (0.25)	Median (2×2)	
	0.76	0.45	
	0.37	0.38	

Rotation means that the image rotates a certain degree. The results measured by NC are presented in Table II.

Wavelet tree quantization (WTQ) [20] is the state-of-art algorithm which achieves prevailing results. To compare the robustness with it, some experiments were done. For fair comparison, Lena is used in the experiments. The results are shown in Table III.

V. CONCLUSION AND FUTURE WORK

In this paper, we have proposed a new method for constructing nontensor product wavelet filter banks and applied them into watermarking scheme design. The new nontensor product wavelet filter banks are constructed according to special symmetric matrix. They overcome the drawback of tensor wavelet banks which can reveal the singularities in the three directions only. Based upon the nontensor filter banks we construct, empirical studies have been conducted to show the capability of nontensor product wavelet filter banks in revealing the singularities in various directions of image. Accordingly, we have developed a modified significant difference watermarking scheme, whose performance shows the superiority of the nontensor product wavelet-based watermarking in terms of robustness and imperceptibility. Further, the proposed wavelet filter banks make the watermarking scheme more flexible because more subbands and coefficients are suitable for watermark embedding.

In addition, a nontensor product wavelet domain watermarking algorithm has been proposed. Experimental results have shown that the proposed algorithm is robust against various attacks. Particularly, regarding Gaussian noising attack, there is a significant improvement in comparison with the tensor wavelets.

As the nontensor product wavelet constructed in this paper can reveal more singularities than the conventional wavelets, it can be applied in many other fields in computer vision and pattern recognition, as well as the digital watermarking. This is

a future direction of our research. In addition, the determination of parameters of nontensor product wavelet is still unknown. We will also work on this problem in the future.

REFERENCES

[1] C. Deng, X.-B. Gao, D.-C. Tao, and X.-L. Li, "Digital watermarking in image affine co-variant regions," in *Proc. Int. Conf. Mach. Learn. Cybern.*, Aug. 2007, vol. 4, pp. 2125–2130.

[2] C. Deng, X. Gao, X. Li, and D. Tao, "Invariant image watermarking based on local feature regions," in *Proc. Int. Conf. Cyberworlds*, Sep. 2008, pp. 6–10.

[3] C. Deng, X. Gao, D. Tao, and X. Li, "Geometrically invariant watermarking using affine covariant regions," in *Proc. IEEE Int. Conf. Image Process.*, Oct. 2008, pp. 413–416.

[4] X. Li, "Watermarking in secure image retrieval," *Pattern Recognit. Lett.*, vol. 24, no. 14, pp. 2431–2434, 2003.

[5] D. Wang and P. Lu, "Geometrically invariant watermark using fast correlation attacks," in *Proc. Int. Conf. Intell. Inf. Hiding Multimedia Signal*, Dec. 2006, pp. 465–468.

[6] I. Pitas, "A method for signature casting on digital images," in *Proc. Int/ Conf. Image Process.*, Sep. 1996, vol. 3, pp. 215–218.

[7] R. B. Wolfgang and E. J. Delp, "A watermark for digital images," in *Proc. Int. Conf. Image Process.*, Sep. 1996, vol. 3, pp. 219–222.

[8] I. J. Cox, J. Kilian, F. T. Leighton, and T. Shamoon, "Secure spread spectrum watermarking for multimedia," *IEEE Trans. Image Process.*, vol. 6, no. 12, pp. 1673–1687, Dec. 1997.

[9] D. Kundur and D. Hatzinakos, "A robust digital image watermarking scheme using the wavelet-based fusion," in *Proc. Int. Conf. Image Process.*, 1997, vol. 4, pp. 544–547.

[10] D. Kundur and D. Hatzinakos, "Digital watermarking using multiresolution wavelet decomposition," in *Proc. IEEE Int. Conf. Acoust., Speech Signal Process.*, May 1998, vol. 5, pp. 2969–2972.

[11] M. Barni, F. Bartolini, and A. Piva, "Improved wavelet-based watermarking through pixel-wise masking," *IEEE Trans. Image Process.*, vol. 10, no. 5, pp. 783–791, May 2001.

[12] X.-G. Xia, C. G. Boncelet, Jr., and G. R. Arce, "A multiresolution watermark for digital images," in *Proc. Int. Conf. Image Process.*, 1997, vol. 4, pp. 548–551.

[13] R. Dugad, K. Ratakonda, and N. Ahuja, "A new wavelet-based scheme for watermarking images," in *Proc. Int. Conf. Image Process.*, 1998, vol. 5, pp. 419–423.

[14] L. Xie and G. R. Arce, "Joint wavelet compression and authentication watermarking," in *Proc. Int. Conf. Image Process.*, 1998, vol. 5, pp. 427–431.

[15] C.-T. Hsu and J.-L. Wu, "Multiresolution watermarking for digital images," *IEEE Trans. Circuits Syst. II, Analog Digit. Signal Process.*, vol. 45, no. 8, pp. 1097–1101, Aug. 1998.

[16] *An efficient watermarking technique using adew and cbwt for copyright protection*. New York: Springer-Verlag, 2006, vol. 4456, pp. 634–641.

[17] Y. Huang, M.-S. Hsieh, and D.-C. Tseng, "Hiding digital watermarks using multiresolution wavelet transform," *IEEE Trans. Ind. Electron.*, vol. 48, no. 5, pp. 875–882, Oct. 2001.

[18] M.-J. Tsai and C.-L. Lin, "Constrained wavelet tree quantization for image watermarking," in *Proc. IEEE Int. Conf. Image Process.*, 2004, pp. 3415–3418.

[19] H.-J. M. Wang, "Multithreshold wavelet codec (MTWC) and perceptual digital watermark casting," Ph.D. dissertation, Univ. Southern California, Los Angeles, CA, 1998.

[20] S.-H. Wang and Y.-P. Lin, "Wavelet tree quantization for copyright protection watermarking," *IEEE Trans. Image Process.*, vol. 13, no. 2, pp. 154–165, Feb. 2004.

[21] W.-H. Lin, S.-J. Horng, T.-W. Kao, P. Fan, C.-L. Lee, and Y. Pan, "An efficient watermarking method based on significant difference of wavelet coefficient quantization," *IEEE Trans. Multimedia*, vol. 10, no. 5, pp. 746–757, May 2008.

[22] R. B. Wolfgang, C. Podilchuk, and E. J. Delp, "The effect of matching watermark and compression transforms in compressed color images," in *Proc. Int. Conf. Image Process.*, 1998, vol. 5, pp. 440–444.

[23] M.-S. Hsieh and D.-C. Tseng, "Wavelet-based color image watermarking using adaptive entropy casting," in *Proc. IEEE Int. Conf. Multimedia Expo*, 2006, pp. 1593–1596.

[24] X. Sun, Z. Wang, and D. Zhang, "A Watermarking Algorithm Based on Ma and DWT," in *Proc. Int. Symp. Electron. Commerce Security*, 2008, pp. 916–919.

[25] G. C. Langelaar and R. L. Lagendijk, "Optimal differential energy watermarking of dct encoded images and video," *IEEE Trans. Image Process.*, vol. 10, no. 1, pp. 148–158, Jan. 2001.

[26] X. You and Y. Y. Tang, "Wavelet-based approach to character skeleton," *IEEE Trans. Image Process.*, vol. 16, no. 5, pp. 1220–1231, May 2007.

[27] A. Cohen and I. Daubechies, "On the instability of arbitrary biorthogonal wavelet packets," *SIAM J. Math. Anal.*, vol. 24, no. 5, pp. 1340–1354, 1993.

[28] R. G. Baraniuk, I. W. Selesnick, and N. G. Kingsbury, "The dual-tree complex wavelet transform," *IEEE Signal Process. Mag.*, vol. 22, no. 6, pp. 123–151, Nov. 2005.

[29] D. Van De Vile and M. Unser, "Complex wavelet bases, steerability, and the marr-like pyramid," *IEEE Trans. Image Process.*, vol. 17, no. 11, pp. 2063–2080, Nov. 2008.

[30] H.-J. Wang and C.-C. J. Kuo, "Image protection via watermarking on perceptually significant wavelet coefficients," in *Proc. IEEE 2nd Workshop Multimedia Signal Process.*, Dec. 1998, pp. 279–284.

[31] M. Alghoniemy and A. H. Tewfik, "Geometric invariance in image watermarking," *IEEE Trans. Image Process.*, vol. 13, no. 2, pp. 145–153, Feb. 2004.

[32] C.-T. Kuo and S.-C. Cheng, "Fusion of color edge detection and color quantization for color image watermarking using principal axes analysis," *Pattern Recognit.*, vol. 40, no. 12, pp. 3691–3704, 2007.

[33] J. Kovacevic and M. Vetterli, "Nonseparable multidimensional perfect reconstruction filter banks and wavelet bases for r^n," *IEEE Trans. Inf. Theory*, vol. 38, no. 2, pt. 2, pp. 533–555, Mar. 1992.

[34] D. Tao and X. Tang, "Nonparametric discriminant analysis in relevance feedback for content-based image retrieval," in *Proc. IEEE Int. Conf. Pattern Recognit.*, Aug. 2004, vol. 2, pp. 1013–1016.

[35] D. Tao, X. Tang, X. Li, and X. Wu, "Asymmetric bagging and random subspace for support vector machines-based relevance feedback in image retrieval," *IEEE Trans. Pattern Anal. Mach. Intell.*, vol. 28, no. 7, pp. 1088–1099, Jul. 2006.

[36] T. Zhang, D. Tao, X. Li, and J. Yang, "Patch alignment for dimensionality reduction," *IEEE Trans. Knowl. Data Eng.*, vol. 21, no. 9, pp. 1299–1313, Sep. 2009.

[37] T. Zhang, D. Tao, and J. Yang, "Discriminative locality alignment," in *Proc. 10th Eur. Conf. Comput. Vis.*, 2008, pp. 725–738.

[38] X. Gao, W. Lu, D. Tao, and X. Li, "Image quality assessment based on multiscale geometric analysis," *IEEE Trans. Image Process.*, vol. 18, no. 7, pp. 1409–1423, Jul. 2009.

[39] Y. Huang, K. Huang, L. Wang, D. Tao, T. Tan, and X. Li, "Enhanced biologically inspired model," in *Proc. IEEE Conf. Comput. Vis. Pattern Recognit.*, Jun. 2008, pp. 1–8.

[40] Q. He, X. You, L. Cui, and Z. Bao, "Watermarking technique based on discrete non-separable wavelet filters," in *Proc. IEEE Int. Conf. Syst., Man Cybern.*, Oct. 2007, pp. 3577–3582.

[41] A. Croisier, D. Esteban, and C. Galand, "Perfect channel splitting by use of interpolation decimation tree decomposition techniques," in *Proc. Conf. Inf. Sci. Syst.*, 1976, pp. 443–446.

[42] P. P. Vaidyanathan, *Multirate Systems and Filter Banks*. Upper Saddle River, NJ: Prentice-Hall, 1993.

[43] M. Vetterli, "Filter banks allowing perfect reconstruction," *Signal Process.*, vol. 10, no. 3, pp. 219–244, 1986.

[44] I. Daubechies, *Ten Lectures on Wavelets*. Philadelphia, PA: Society Industrial Appl. Math., 1992.

[45] A. Cohen and I. Daubechies, "Non-separable bidimensional wavelet bases," *Revista Matemática Iberoamericana*, vol. 9, no. 1, pp. 51–137, 1993.

[46] S. D. Riemenschneider, R. Q. Jia, and D. X. Zhou, "Smoothness of multiple refinable functions and multiple wavelets," *SIAM J. Math. Anal.*, vol. 21, pp. 1–28, 1999.

[47] A. S. Cavaretta, W. Dahmen, and C. A. Micchelli, "Stationary subdivision," *Memoirs Amer. Math. Soc.*, vol. 93, no. 453, pp. 1–186, 1991.

[48] W. Dahmen and C. A. Micchelli, "Biorthogonal wavelet expansions," *Construct. Approx.*, vol. 13, pp. 293–328, 1997.

[49] S. Mallat, *Wavelet Tour of Signal Processing*. San Diego, CA: Academic, 1998.

[50] F. A. P. Petitcolas, "Weakness of existing watermark scheme," [Online]. Available: http://www.petitcolas.net/fabien/watermarking/stirmark/index.html

[51] Ulead system, Inc., PhotoImpact 13. Software [Online]. Available: http://www.ulead.com

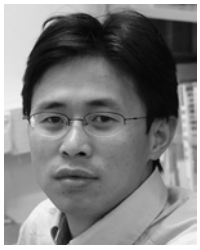

Xinge You (M'08–SM'10) received the B.S. and M.S. degrees in mathematics from the Hubei University, Wuhan, China, in 1990, and the Ph.D. degree in computer science from the Hong Kong Baptist University, Hong Kong, in 2000 and 2004, respectively.

He is presently a Professor in the Department of Electronics and Information Engineering, Huazhong University of Science and Technology, Wuhan, China. His current research interests include wavelets and its application, signal and image processing, pattern recognition, machine learning, and computer vision.

Liang Du (S'08–M'09) recieved the B.S. degree from School of Electronic and Information, Wuhan University, Wuhan, China, in 2008, and is currently pursuing the M.S. degree in the Department of Electronics and Information Engineering, Huazhong University of Science and Technology, Wuhan, China.

His research interests include image processing and computer vision.

Yiu-ming Cheung (SM'06) received the Ph.D. degree from the Department of Computer Science and Engineering, The Chinese University of Hong Kong in 2000.

He joined the Department of Computer Science at Hong Kong Baptist University in 2001, and then became an Associate Professor in 2005. His current research interests are in the fields of machine learning and information security, particularly the topics on clustering analysis, blind source separation, neural networks, nonlinear optimization, watermarking and lip-reading. He is the founding Chairman of IEEE (Hong Kong) Computational Intelligence Chapter.

Dr. Cheung is a Senior Member of ACM. He has taken the key positions (e.g., Organizing Committee Chair, Programme Committee Chair, Financial Chair etc.) in several major international conferences, including The 2006 IEEE International Conference on Data Mining (ICDM 2006) and The 2006 IEEE/WIC/ACM International Joint Conferences on Web Intelligence and Intelligent Agent Technology (WI-IAT 2006). Currently, he is the Associate Editor of *Knowledge and Information Systems*, as well as the guest co-editor and editorial board member of the several international journals.

Qiuhui Chen received the Ph.D. degree from the Institute of Mathematics, Chinese Academy of Sciences, Beijing, China, in 1996.

He is currently a Professor in the School of Informatics, Guangdong University of Foreign Studies, Guangzhou, China. His research interest include time-frequency analysis and signal processing.